Microchemical Journal 130 (2017) 442–451

Contents lists available at ScienceDirect

Microchemical Journal

journal homepage: www.elsevier.com/locate/microc

Novel extractant impregnated resin for preconcentration and determination of uranium from environmental samples

Sandesh R. Tetgure [a], Bharat C. Choudhary [a], Dipak J. Garole [a,b,*], Amulrao U. Borse [a,*], Arun D. Sawant [c], Surendra Prasad [d,*]

[a] School of Chemical Sciences, North Maharashtra University, Jalgaon 425001, Maharashtra, India
[b] Directorate of Geology and Mining, Government of Maharashtra, Nagpur 440010, Maharashtra, India
[c] Inorganic Chemistry Division, The Institute of Science, 15 Madam Kama Road, Mumbai 400032, Maharashtra, India
[d] School of Biological and Chemical Sciences, Faculty of Science, Technology and Environment, The University of the South Pacific, Private Mail Bag, Suva, Fiji

ARTICLE INFO

Article history:
Received 1 October 2016
Accepted 7 October 2016
Available online 20 October 2016

Keywords:
Uranium determination
Isonitroso-4-methyl-2-pentanone
Amberlite XAD-4
Solid phase extraction
Uranium recovery

ABSTRACT

A novel method based on impregnation of Amberlite XAD-4 with extractant isonitroso-4-methyl-2-pentanone (IMP) has been developed for U^{6+} extraction and determination in various samples. The prepared extractant impregnated resin (EIR) sorbent was characterized by the field emission scanning electron microscope. The sorbent was packed in a glass column and investigated for various parameters such as pH, eluent, sample and eluent flow rates to optimize sorption desorption conditions for U^{6+}. U^{6+} is quantitatively determined at pH 4 with flow rate 2 mL/min which showed recovery of 98.9%. The sorption behaviour of U^{6+} by EIR was also studied using different equilibrium isotherms and kinetic models and the experimental data confirmed that it follows Freundlich isotherm and Weber-Morris pore diffusion kinetic model. The investigation of foreign ions influence on U^{6+} sorption showed least interference and thus, facilitated its extraction and determination in Uranmicrolite (leachate) ore tailing, synthetic mixtures and spiked water samples. The detection limit was 0.41 μg/L while the limit of quantification as 1.35 μg/L made the method quite accurate.

1. Introduction

Uranium is one of the most hazardous elements to the environment due to its radioactivity and toxicity [1,2]. Now a days, separation and determination of uranium is gaining more importance due to its increasing applications in different fields such as nuclear energy generation, manufacture of nuclear weapons, shielding of industrial radioactive sources, anti-tanks ammunition, catalysts, staining pigments, burning of fossil fuel (oil and coal) and uranium containing phosphate minerals [3–5]. Uranium can cause non-malignant respiratory disease (fibrosis, emphysema), nephrotoxicity [6] and the target organ to be considered for uranium toxicity is mainly kidney [7]. Uranium is one of the heaviest naturally occurring elements and is found at an average concentration of 0.0004% in the Earth's crust [8]. Seawater contains around 3 μg/L of uranium and is distributed uniformly in all the World's oceans [9]. In most countries, the tolerance level for uranium in drinking water as described by the United States Environmental Protection Agency (USEPA) is 0.03 mg/L [10]. Therefore, in view of its toxicity, occurrence and potential uses, it is desirable to develop sensitive and reliable analytical methods to detect or remove trace concentrations of uranium from different samples.

Several methods have been developed for the detection and determination of uranium at trace and ultra-trace levels [3,8,11–17]. However, to achieve high sensitivity by minimizing effects of the matrix caused by commonly present interfering ions, separation and/or preconcentration procedure is required to be developed prior to the analysis of uranium [3]. Various methods available for preconcentration and separation of uranium are: liquid-liquid extraction [18–20], ion-exchange [21,22], solid phase extraction (SPE) [23–27], ion imprinting polymers [28–30] and cloud point extraction and determination [31,32]. Recently, SPE has increasingly been used for preconcentration, separation and removal of trace and ultra-trace amounts of uranium species from complex matrices [33–36]. Rao et al. have presented an overview of the preconcentration techniques used prior to the determination of U^{6+} [11]. While, Kim et al., have reviewed the methods for the recovery of uranium from sea water [13].

Polymeric resins have also been used as solid support after the modification of their surface by binding different reagents. Amberlite XAD resin series (polystyrene-divinyl benzene) such as Amberlite XAD-1, XAD-2, XAD-4 and XAD-16 has high hydrophobic character and no ion-exchange capacity. However, these resins are quite important from both the economical and environmental points of view for SPE after their proper modifications [37]. Surface modification of Amberlite

* Corresponding authors.
E-mail addresses: drdipakgarole@gmail.com (D.J. Garole), amulborse@gmail.com (A.U. Borse), prasad_su@usp.ac.fj (S. Prasad).

http://dx.doi.org/10.1016/j.microc.2016.10.019
0026-265X/

XAD resin is an easy and economical choice for the separation and preconcentration of metal ions from aqueous samples [38]. These surface modifications can be done either by chemically binding a selective reagent to the solid support or by impregnating it physically on solid support. Out of these two processes, physical impregnation is relatively simple and easy process for preparation of solid phases. Impregnated resins are considered as chelating resins whose functional groups are not chemically bounded to the matrix but physically adsorbed on it. Literature survey revealed the determination of uranium using solvent impregnated resin (SIR) [39–42]. Although extractant impregnated resin (EIR) gives added advantage over SIR in terms of reusability due to minimum leaching as a result of strong binding of extractant, some research has been carried on EIR [43–47].

In continuation of our work in the field of radioactive elements [48, 49], herein we present a systematic investigation for sorption and desorption of U^{6+} on a column packed with Amberlite XAD-4 impregnated with isonitroso-4-methyl-2-pentanone (IMP) as well as its batch study in terms of different kinetic and isotherm models. The impregnation of IMP on Amberlite XAD-4 characterized by FE-SEM and investigated systematically to devise the optimum conditions for determination and recovery of U^{6+} from variety of real samples like Uranmicrolite (leachate) ore tailing, synthetic mixtures and spiked water.

2. Materials and methods

2.1. Materials

Amberlite XAD-4 resin (20–60 mesh size) was purchased from Supelco, Sigma Aldrich and pre-treated by washing sequentially with methanol, double distilled water (DDW), 1 M HNO_3, DDW, 1 M Noah and finally with DDW to remove impurities [40]. Stock solution of 2.5 mg/mL U^{6+} was prepared by dissolving appropriate quantity of uranium nitrate hexahydrate ($UO_2(NO_3)_2 \cdot 6H_2O$) obtained from British Drug House Ltd. (India) in slightly acidified DDW. The stock solution of U^{6+} was standardized gravimetrically [50], and a working solution containing 30 μg/mL of U^{6+} was prepared by appropriate dilution. Arsenazo(III) was procured from S.D. Fine Chemicals (India) and its aqueous solution 0.1% (w/v) was prepared for spectrophotometric determination of U^{6+}. All reagents used were AR grade.

2.2. Instrumentation

For morphological characterization of EIR, the FE-SEM monographs were recorded using S-4800 instrument of Hitachi (Japan) at accelerating voltage of 20 kV. Before recording FE-SEM images, EIR was made conductive by coating gold layer using an ion sputter coater instrument model E-1010, Hitachi (Japan). A Shimadzu electronic balance BL-220H (Japan) was used for weighing. A Systronics digital pH meter 335 with a combined glass electrode was used for measuring pH of the solution during experiments. A Shimadzu 2450 UV–visible spectrophotometer with 1 cm quartz cell was used for spectrophotometric determination of U^{6+}. A glass column (150 mm × 10 mm, J-Sil, India) was used for column studies. An orbital shaker model BTI 39 (Bio-Technics, India) was used throughout the experiments.

2.3. Preparation of EIR sorbent

EIR was prepared by using our method reported elsewhere [48]. Then EIR was subjected to several batch adsorption-desorption cycles (10 cycles) for U^{6+}.

2.3.1. Experimental for column method

Glass column with dimensions of 150 mm length and 10 mm inner diameter was packed uniformly with 100 mg of EIR having glass wool as supports. The packed column was preconditioned with 20–25 mL of pH 4 solution adjusted with dilute HNO_3. After preconditioning, extraction was performed by passing 25 mL aqueous solution of 1.2 μg/mL U^{6+} at pH 4 with optimum flow rate of 2 mL/min. The extracted U^{6+} was then desorbed from the column using 10 mL of 1 M HCl at 0.2 mL/min flow rate and recovered U^{6+} was spectrophotometrically determined with arsenazo(III) at 650 nm [51]. The optimized conditions of column studies for the extraction and quantification of U^{6+} are tabulated in Table 1. All the experiments were carried out in triplicate.

2.3.2. Experimental for batch method

In batch method, initially 100 mg of EIR was preconditioned with 25 mL of pH 4 solution of dilute HNO_3 in 250 mL stoppered glass bottles (shaking vessels). Then 25 mL solutions containing appropriate amounts (100 μg to 20 mg) of U^{6+} was sorbed by preconditioned EIR. The sorption was performed for 50 min at 100 rpm and then EIR was allowed to settle for 10 min. The settled EIR was separated from aqueous phase using Whatman filter paper (no. 42). The filtered out EIR corresponding to different concentration range were transferred to different shaking vessels. The extracted U^{6+} was recovered using 10 mL of 1 M HCl by shaking for 30 min at 50 rpm. Then the amounts of U^{6+} before and after extraction were determined spectrophotometrically with arsenazo(III) at 650 nm [51]. All experiments were performed in triplicate. Different parameters like stirring speed, concentration and contact time were studied for U^{6+} sorption. The amount of U^{6+} adsorbed i.e. q_t mg/g of EIR at time t was calculated using Eq. (1) where C_0 and C_t are the initial and liquid-phase concentrations of U^{6+} (mg/L), respectively at t, V is the volume of U^{6+} solution (L) and m is the mass of EIR (g).

$$q_t = (C_0 - C_t)\,V/m \tag{1}$$

3. Results and discussion

3.1. FE-SEM analysis

The prepared EIR was characterized as reported in our earlier communication [48]. The impregnation of IMP on/in polymeric resin Amberlite XAD-4 was confirmed by morphological characterization of EIR using FE-SEM analysis. The FE-SEM images of the pre-treated Amberlite XAD-4 resin (before impregnation) and EIR (after impregnation) were studied and are shown in Fig. 1. The fractures seen on the surface of pre-treated Amberlite XAD-4 (Fig. 1a, b, c) were due to the initial acidic and basic pre-treatment given to the resin for purification. The impregnation resulted in systematic covering of resin by extractant forming net structure on the surface of resin in nano-range (Fig. 1d, e, f).

Table 1
Optimized parameters for sorption and quantification of U^{6+} by EIR.

Parameters	Optimum condition
Aqueous phase pH	4.0
Flow rate for sorption (mL/min)	2.0
[HCl] for desorption (M)	1.0
Flow rate for desorption (mL/min)	0.2
Preconcentration factor	150
Breakthrough volume (mL)	≥1500
RSD (%)	≤1.6
Average recovery (%)	98.9
LOD (μg/L)	0.41
LOQ (μg/L)	1.35
Reusability (cycles)	80
λ_{max} (nm)	650

RSD: Relative standard deviation, LOD: Limit of detection, LOQ: Limit of quantification.

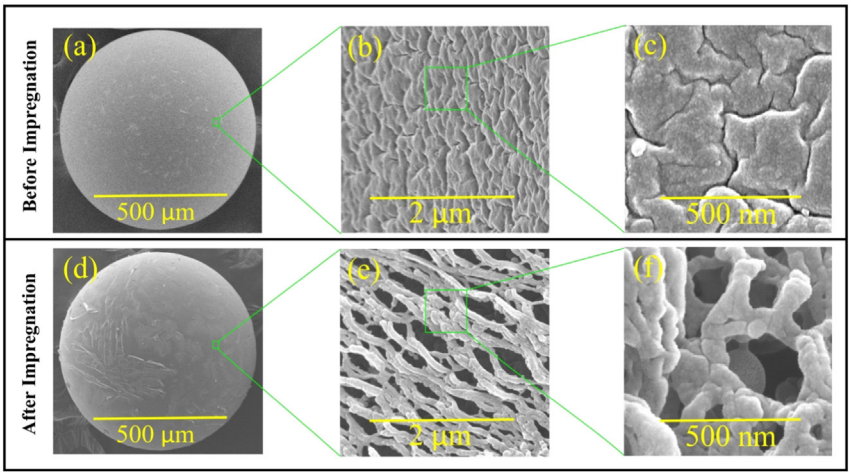

Fig. 1. FE-SEM images at different magnifications; (a) Bead of pre-treated Amberlite XAD-4 resin at 500 μm (b) surface of pre-treated Amberlite XAD-4 resin at 2 μm (c) surface of pre-treated Amberlite XAD-4 resin at 500 nm before impregnation (d) Bead of EIR at 500 μm (e) surface of EIR at 2 μm and (f) surface of EIR at 500 nm after impregnation.

3.2. Extraction mechanism

The extractant IMP consists of hydrophilic head (electron rich centre) and hydrophobic tail (carbon frame). As Amberlite XAD-4 resin was hydrophobic in nature, hydrophobic tail arranged itself on the wall and in the pores of resin so that hydrophilic head of extractant remained free for extraction purpose [48]. When resin containing free hydrophilic head came in contact with aqueous phase containing electron deficient analyte at desire pH, head formed complex with analyte and resulted in extraction. Fig. 2 shows the schematic illustration of possible extraction mechanism.

3.3. Column studies

In the column study, the effects of analytical parameters on the extraction of U^{6+} were investigated sequentially for optimization. Then, the same optimized conditions for the column method were applied to the batch method.

3.3.1. Effect of pH on sorption

pH is an important parameter in aqueous phase study because the sorption behaviour is pH dependant. Therefore, the sorption of U^{6+} on the columns containing EIR sorbent was studied in the pH range 1–8 and the results are presented in Fig. 3a. Initially, U^{6+} sorption increased with the increasing pH and it was quantitative between pH 4–6. It observed that plain Amberlite XAD-4 resin sorption of U^{6+} was negligible (<5%). It indicates that impregnation of IMP on Amberlite XAD-4 resin is necessary for sorption of U^{6+}. pH 4 was considered for the optimum pH used for further studies.

To understand the reason of U^{6+} soption in the range of pH 4–6 it was necessary to study absorbance of 0.01 M IMP at its λ_{max} (312 nm in 95% v/v acetonitrile-water) at different pH range 2–8 [52] and the results are shown in Fig. 3b. The IMP showed the maximum absorbance in pH range of about 3.5–6 which suggested that in this pH range extractant IMP remains in its six membered ring form as shown in Fig. 2. Also, the sorption of U^{6+} was quantitative between pH 4–6 which suggested that six membered ring of IMP was responsible for the sorption of U^{6+} by EIR. Therefore, the sorption of U^{6+} proceeds through complex formation between six membered ring of IMP and U^{6+}.

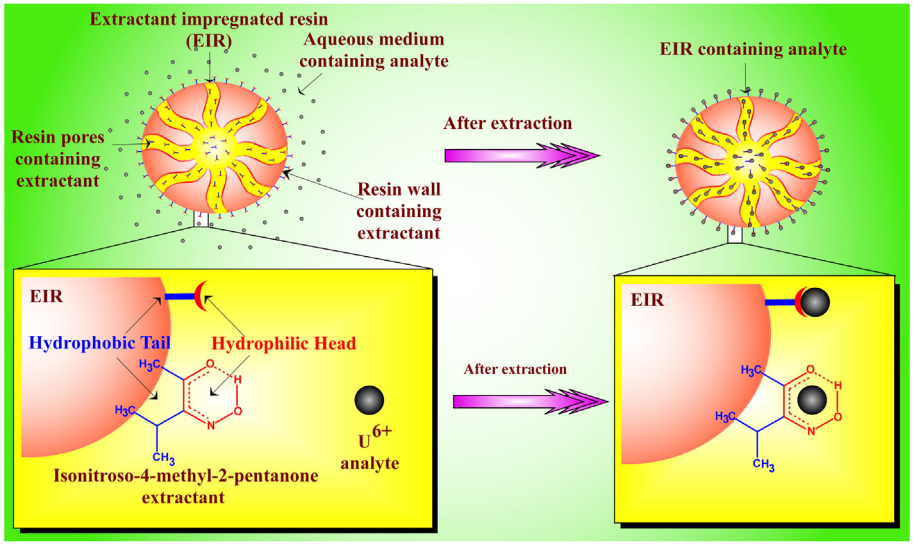

Fig. 2. Schematic illustration of possible extraction mechanism.

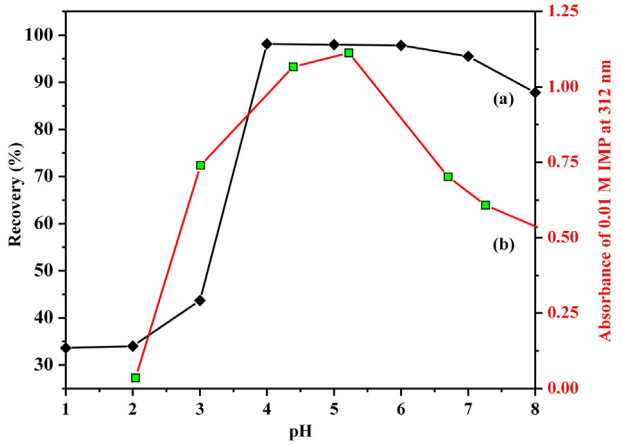

Fig. 3. (a) Effect of aqueous phase pH on the sorption of U^{6+} (% recovery) under the experimental conditions: 25 mL containing 30 μg U^{6+}, flow rate 2 mL/min and eluent; 10 mL of 1 M HCl, flow rate 0.2 mL/min (b) Absorbance values of 0.01 M IMP at 312 nm with variation on pH.

3.3.2. Aqueous phase flow rate and volume

Optimization of flow rate is an important parameter as it relates to the speed of analysis but high flow rate could result in incomplete analyte transfer from liquid phase to solid phase. Thus, to optimize this parameter, aqueous flow rate was varied from 0.5 to 3.5 mL/min and results are shown in Fig. 4. It was observed that U^{6+} was almost quantitatively sorbed when flow rate was 0.5 to 2.5 mL/min sample while at flow rate > 2.5 mL/min sorption of U^{6+} decreased. Hence, sample flow rate of 2 mL/min was chosen and used in all subsequent studies.

The sample volume related to preconcentration factor is extremely important in any SPE methodology. Thus, different volumes of sample solution (50–2000 mL) containing 30 μg U^{6+} were passed through the column at pH 4 and U^{6+} recovery studies were carried out. The results shown in Fig. 5. clearly show that the recoveries of U^{6+} were quantitative (99.7 ± 0.6%) from 50 to 1500 mL of sample volume containing 30 μg U^{6+}. Preconcentration factor is the ratio of the maximum aqueous volume (mL) from which analyte can be quantitatively recovered to the volume of eluent (mL) used for desorption of analyte. Therefore preconcentration factor for developed method was found to be 150, as eluent volume was 10 mL.

3.3.3. Optimization of eluent phase parameters

The recovery of U^{6+} from EIR was optimized by evaluating different parameters as shown in Table 2. The recovery of 99.1 ± 0.2% was accomplished with 10 mL of 1 M HCl at a flow rate of 0.2 mL/min. The

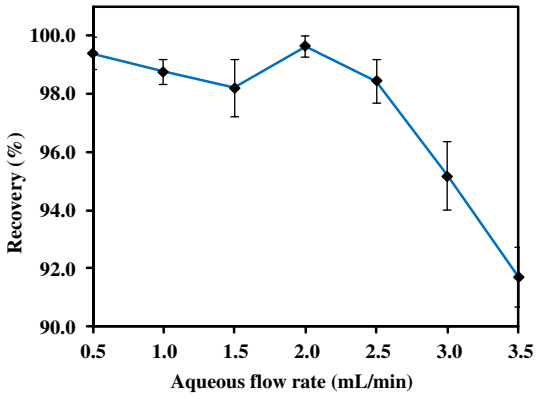

Fig. 4. Effect of aqueous phase flow rate on the sorption of U^{6+} (% recovery) under the experimental conditions: 25 mL containing 30 μg U^{6+}, pH 4 and eluent; 10 mL of 1 M HCl, flow rate 0.2 mL/min.

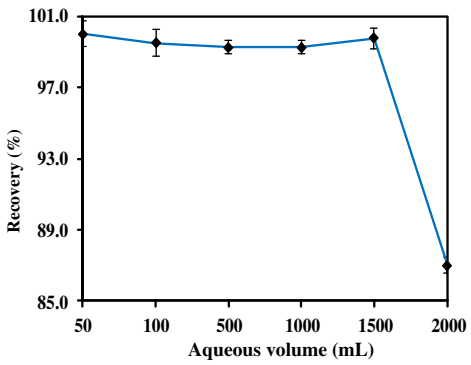

Fig. 5. Effect of volume on the sorption of U^{6+} (% recovery) under the experimental conditions: 25 mL containing 30 μg U^{6+}, pH 4, flow rate 2 mL/min and eluent; 10 mL of 1 M HCl, flow rate 0.2 mL/min.

eluent volume was varied in the range 5–15 mL of 1 M HCl. It was found that 5 mL of 1 M HCl resulted in 86.0 ± 0.7% recovery whereas 10 mL and 15 mL of 1 M HCl showed recovery of 99.6 ± 0.4 and 99.4 ± 0.4% respectively. Hence the effect of eluent flow rate was examined from 0.2–0.6 mL/min with 10 mL of 1 M HCl. The recovery 99.1 ± 0.2% was achieved at 0.2 mL/min flow rate while at higher flow rates the recovery of U^{6+} decreased as shown in Table 2. Therefore, 10 mL of 1 M HCl at a flow rate of 0.2 mL/min was used as an eluent for all subsequent studies.

3.3.4. Stability test of column

The reusability of the extraction column is the major advantage of SPE as it suggests the number of successive analyses feasible without changing the column packing. The stability and reusability of the EIR packed column was evaluated by observing the recovery of U^{6+} through several sorption - desorption cycles using the same column. To assess this parameter, 25 mL sample solution containing 30 μg U^{6+} was passed through the column and desorbed with 10 mL of 1 M HCl. The recovery results are shown in Fig. 6. It was observed that column was stable up to 80 cycles with a 97.9 ± 0.2% recovery of U^{6+}. This study confirmed a very high reusability and reliability of the EIR for continuous usage.

3.3.5. Effect of foreign ions

Real samples contain matrix of foreign ions which may interfere in the analysis of targeted ion. Therefore, setting the maximum tolerance limits for commonly present ions in sample matrix is necessary. In this context, a known different amounts of foreign ion was added to 25 mL of aqueous sample solution containing 30 μg of U^{6+}, and recovery study was carried out by the developed procedure. The tolerance limit was set as the maximum concentration of the foreign ions which cause an approximately ±2% relative error in the quantitative

Table 2
Summary of eluent phase parameters study.

Eluent phase parameter	Recovery of U^{6+} (%) ± RSD
[HCl] (M)	
0.5	94.6 ± 0.8
1.0	99.1 ± 0.2
2.0	99.6 ± 0.4
HCl volume (mL)	
5.0	86.0 ± 0.7
10.0	99.6 ± 0.4
15.0	99.4 ± 0.4
Flow rate (mL/min)	
0.2	99.1 ± 0.2
0.4	97.5 ± 0.2
0.6	97.0 ± 0.4

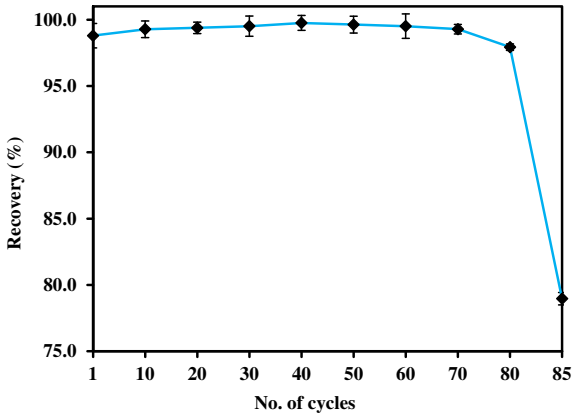

Fig. 6. Stability test of column under the experimental conditions: 25 mL containing 30 μg U^{6+}, pH 4, flow rate 2 mL/min and eluent; 10 mL of 1 M HCl, flow rate 0.2 mL/min.

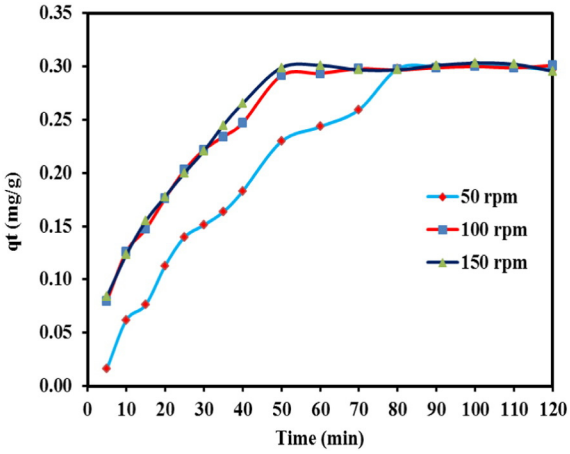

Fig. 7. Effect of contact time (5–120 min) and stirring speed (50, 100, 150 rpm) on U^{6+} sorption at 298 K under the experimental conditions: 25 mL containing 30 μg U^{6+}, pH 4 and eluent; 10 mL of 1 M HCl.

determination and recovery of U^{6+}. The results obtained are shown in Table 3. The alkali and alkaline earth metal ions showed high tolerance limit in the range 5500–2000 μg. Some *p*-block and *d*-block cations showed the tolerance limit in the range 1500–300 μg. Inorganic, organic and some other anions had the tolerance limit in the range 5000–150 μg. Other cations (rare earths) showed the tolerance limit in the range 120–30 μg. V^{4+}, Fe^{3+} has shown serious interference in U^{6+} sorption when present at 20 μg concentration.

3.4. Batch studies

3.4.1. Optimization of batch parameters

The batch parameters like contact time and stirring speed were optimized for U^{6+} sorption on EIR. Fig. 7 shows the effect of contact time studied in the range 5–120 min and at stirring speed of 50, 100, 150 rpm for U^{6+} extraction at pH 4 with initial concentration of 1.2 μg/mL. The adsorption increased with increase in time and stirring speed. It was observed that with 50 rpm stirring speed, the equilibrium reached at 80 min while at 100 and 150 rpm it required only 50 min to reach equilibrium. This is due to the fact that slower shaking speed decreased the suspension of all resin particles which decreased contact time between solid surface and liquid phase and resulted in decrease in transfer of U^{6+} to active sites of EIR surface. However, increase in stirring speed up to 150 rpm has not shown significant effect on equilibrium time (50 min). Therefore, stirring speed of 100 rpm and contact time of 50 min were taken as optimized parameters for further study.

3.4.2. Kinetic behaviour

The kinetic parameters were calculated by fitting the experimental data to different kinetic models; such as Lagergren pseudo first order, Lagergren pseudo second order, Elovich model and Weber-Morris pore diffusion model which are described below [53–57] and results of these models are given in Table 4.

In the Lagergren pseudo first order model, the sorption velocity is proportional to the concentration of the adsorbate [53]. The linearized form of pseudo first order kinetic equation is expressed in Eq. (2) [54] where q_e (mg/g) and q_t (mg/g) are U^{6+} amount adsorbed in the equilibrium and at any time t, respectively and k_1 is the Lagergren rate constant (min^{-1}).

$$log(q_e - q_t) = (log q_e) - (k_1 t/2.303) \quad (2)$$

The plot of log ($q_e - q_t$) against time t at 298 K is shown in Fig. 8a which shows the kinetic sorption behaviour of U^{6+} from aqueous solution using EIR. The results fitted well to this model with R^2 value was found to be 0.9948. Calculated values of q_e and K_1 were 1.371 mg/g and 0.043 min^{-1} (Table 4).

The linearized form of Lagergren pseudo second order adsorption kinetic model is expressed in Eq. (3) [55] where k_2 is the rate constant of pseudo second order adsorption (g mg^{-1} min^{-1}). The plot of (t/q_t) versus t shown in Fig. 8b was used to calculate the values of k_2 and q_e and as

Table 3
Interference study of some commonly coexisting ions on the sorption of U^{6+} by EIR under the experimental conditions: 25 mL containing 30 μg U^{6+}, pH 4, flow rate 2 mL/min and eluent; 10 mL of 1 M HCl, flow rate 0.2 mL/min.

Foreign ion	Tolerance limit (μg)	Foreign ion	Tolerance limit (μg)	Foreign ion	Tolerance limit (μg)
Cations		Other cations		Anions	
K^+	5500	Dy^{3+}	120	$EDTA^{4-}$	5000
Na^+, Mg^{2+}	5000	La^{3+}	100	Br^-	1000
Ca^{2+}	4500	Gd^{3+}	60	SO_4^{2-}	500
Ba^{2+}	4000	Sc^{3+}, Y^{3+}	30	Oxalate ($C_2O_4^{2-}$)	400
Sr^{2+}	2000	Ce^{4+}	30	ClO_4^-	250
Pb^{2+}, Mn^{2+}, Zn^{2+}, Cd^{2+}, V^{5+}	1500	Pr^{3+}	30	Tartrate ($C_4H_4O_6^{2-}$)	200
Cr^{3+}	1000	Nd^{3+}	30	SCN^-	200
Cr^{6+}, Ni^{2+}, Sb^{3+}	750	Sm^{3+}	30	Citrate ($C_6H_5O_7^{3-}$)	150
Co^{2+}, Al^{2+}, Nb^{5+}, Ta^{5+}	500	Y^{3+}	30	CH_3COO^-	150
Cu^{2+}	300	Th^{4+}	30 [a]		
V^{4+}, Fe^{3+}	< 20	Zr^{4+}	Co-extracted		

[a] Th^{4+} was masked with 1 mL 0.01 M EDTA.

Table 4
Summarized results of kinetic behaviour.

Lagergren pseudo first order		
q_e (mg/g)	k_1 (min^{-1})	R^2
0.2743	0.043	0.9948
Lagergren pseudo second order		
q_e (mg/g)	k_2 (g mg^{-1} min^{-1})	R^2
0.421	0.090	0.9762
Elovich model		
α (mg/g min^{-1})	β (g mg^{-1})	R^2
0.0375	12.16	0.9813
Weber-Morris pore diffusion		
K_{id} (mg/g $min^{-1/2}$)	–	R^2
0.0395		0.9889

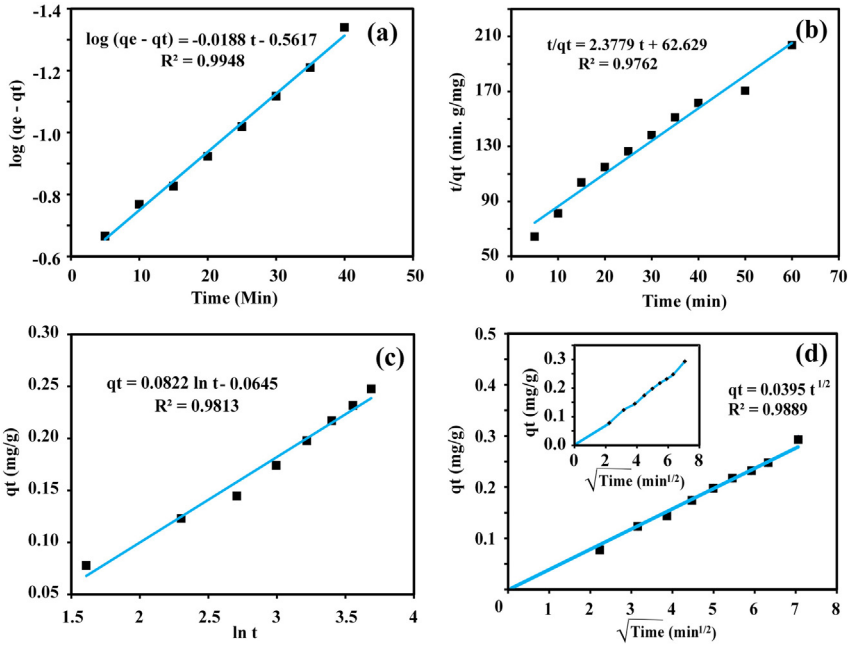

Fig. 8. Different kinetic plot (a) Lagergren pseudo first order, (b) Lagergren pseudo second order, (c) Elovich model and (d) Weber-Morris pore diffusion (inset shows deviation in straight line of Weber-Morris pore diffusion).

0.090 g mg^{-1} min^{-1} and 0.421 mg/g of EIR, respectively (Table 4).

$$(t/q_t) = \left(1/k_2 q_e^2\right) + (t/q_e) \quad (3)$$

Elovich Eq. (4) was derived assuming that the kinetics followed either a diffusion process (inter-particle or intra-particle) or a heterogeneous surface reaction [56] where α (mg/g min^{-1}) is the initial adsorption rate constant and the parameter β (g mg^{-1}) is the extent of surface coverage and activation energy for chemisorption. The values of α and β were calculated from the plot of q_t against ln t as shown in Fig. 8c which were found to be 0.0375 mg/g min^{-1} and 12.16 g mg^{-1}, respectively. The characterization of EIR showed that this EIR was heterogeneous material and good R^2 value (0.9813) also confirms the applicability of Elovich model for this system. Therefore, the extraction process of U^{6+} on/in heterogeneous surface of EIR proceed through chemisorption.

$$q_t = ((1/\beta)\ln(\alpha\beta)) + ((1/\beta)\ln t) \quad (4)$$

Several steps are involved in the sorption of sorbate by a sorbent such as transport of the sorbate from the aqueous phase to the surface of the sorbent and diffusion of the sorbate into the interior of the pores by a slow process. The presence of pore diffusion or internal diffusion and determination whether pore diffusion is the rate determining step in adsorption process is studied by Weber-Morris pore diffusion [57] given by Eq. (5).

$$q_t = k_{id}\left(t^{1/2}\right) + C \quad (5)$$

Here, q_t is the amount adsorbed per unit mass of EIR (mg/g) at time t, k_{id} is the intra-particle diffusion rate constant (mg/g $min^{-1/2}$) and C (mg/g) is a constant. The value of C gives an idea about the boundary layer thickness i.e. greater the value of C, greater is the boundary layer effect. The plot of q_t versus $t^{1/2}$ shown in Fig. 8d resulted in a straight line passing through origin which confirmed that the intra-particle diffusion was involved in the sorption process as the controlling step [57]. The slope of this linear plot gave the value of k_{id} as 0.0395 mg/g $min^{-1/2}$ of EIR for U^{6+}. Small deviation from straight line (inset of Fig. 8d) was observed in time interval of 10 to 20 min was attributed to rapid external diffusion as free sites for sorption were available initially. After 20 min, the Weber-Morris relationship holds good where the linear portion was a consequence of a gradual adsorption stage due to intra-particle diffusion.

3.4.3. Isotherm behaviour

The equilibrium adsorption isotherm is quite important to describe the mechanism of adsorption. Different isotherm models like Langmuir, Freundlich, Temkin and Dubinin-Radushkevich (D-R) were applied to correlate the experimental data [47,53,58–60]. The adsorption isotherms for U^{6+} extraction on EIR were obtained with different concentrations (4–800 mg/L) at constant temperature (298 K). All isotherm parameters have been tabulated in Table 5. Fig. 9a shows experimental results in terms of sorption capacity curve (plot of amount of U^{6+} sorbed per unit weight of EIR at equilibrium concentration, q_e (mg/g) against concentration of U^{6+} loaded (mg/L)).

The Langmuir model assumes that a monolayer sorption occurs at energetically equivalent sites and is given by Eq. (6) [47] where C_e is the equilibrium concentration (mg/L), q_e is the amount of U^{6+} adsorbed at equilibrium (mg/g), q_m the maximum amount of U^{6+} adsorbed corresponding to the complete monolayer coverage (mg/g) and b is the energy of adsorption (Langmuir constant, L/mg). The values of q_m and b as

Table 5
Isotherm parameters obtained from Langmuir, Freundlich, Temkin and D-R models at 298 K.

Langmuir model			
q_m (mg/g)	b (L/mg)		R^2
18.69	0.0097		0.9906
Freundlich model			
K_F (mg/g)	N		R^2
0.455	1.619		0.9965
Temkin model			
B	b (J/mol)	A (L/g)	R^2
11.811	209.9	0.0535	0.9936
D-R model			
q_s (mg/g)	K_{ad} (mol^2/kJ^2)	E (kJ/mol)	R^2
16.44	0.0018	11.79	0.9970

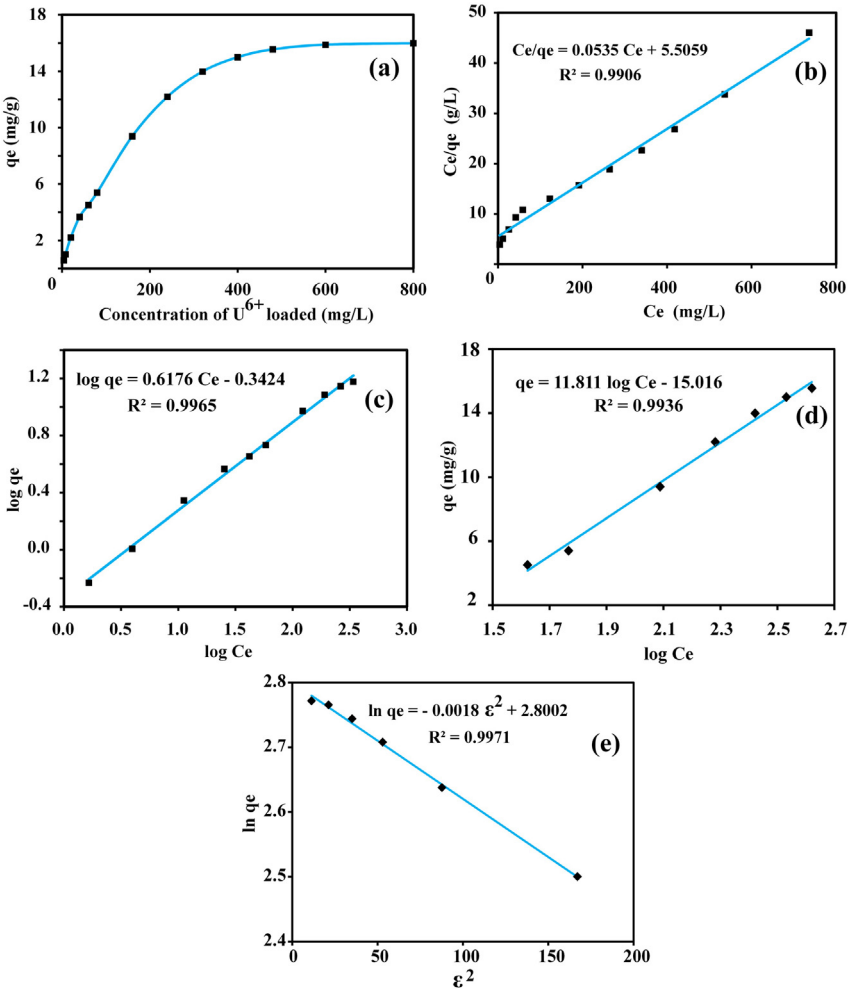

Fig. 9. Different isotherm plots (a) sorption capacity curve and (b) Langmuir (c) Freundlich (d) Temkin and (e) Dubinin-Radushkevich (D-R) models.

18.69 mg/g and 0.0097 L/mg, respectively were calculated from the slope and intercept of the Langmuir linear plot of C_e/q_e versus C_e shown in Fig. 9b. Although the results could be fitted and q_m value calculated; this is not the best model to be used with this EIR, because the Langmuir model is for homogeneous adsorbents and the EIR is a heterogeneous adsorbent according to its characterization.

$$(C_e/q_e) = (1/q_m b) + (C_e/q_m) \quad (6)$$

The Freundlich isotherm model is based on sorption on a heterogeneous surface which assumes that with increased adsorbate concentration in the solution the adsorbate concentration in the adsorbent surface also increases [53]. The linearized logarithmic form of Freundlich model is given by Eq. (7) where K_F and n are Freundlich constants (0.455 mg/g and 1.619, respectively) calculated from the slope and intercept of the plot log q_e versus log C_e (Fig. 9c). The value for n obtained was between 1 and 10 representing a good potential of the EIR.

$$\log q_e = 1/n \log C_e + \log K_F \quad (7)$$

The Temkin model considers the heat of adsorption of molecules on the surface of adsorbent and suggests a linear decrease of sorption energy as the degree of completion of the sorptional centres of an adsorbent is increased [58]. The linearized form of Temkin model is given by Eq. (8) where B = RT/b.

$$q_e = B \log A + B \log C_e \quad (8)$$

The value of b (Temkin constant) is related to heat of sorption (J/mol), R is universal gas constant (8.314 J/mol·K), T is absolute temperature (298.15 K) and A is Temkin isotherm constant (L/g). The sorption

Table 6
Determination and recovery of U^{6+} from some synthetic samples under the experimental conditions: 25 mL containing 30 μg U^{6+} with other matrix added, pH 4, flow rate 2 mL/min and eluent 10 mL of 1 M HCl, flow rate 0.2 mL/min.[a]

Composition of mixture	Recovery of U^{6+} (%) ± RSD
10 μg Y^{3+}, 20 μg V^{5+}, 40 μg La^{3+}, 30 μg U^{6+}	99.2 ± 1.1
30 μg Ca^{2+}, 15 μg Th^{4+} [a], 33 μg Cd^{2+}, 30 μg Pb^{2+}, 30 μg U^{6+}	99.0 ± 1.2
50 μg Mg^{2+}, 10 μg Y^{3+}, 10 μg Th^{4+} [a], 30 μg Al^{2+}, 30 μg U^{6+}	98.9 ± 1.3

[a] Th^{4+} was masked with 1 mL of 0.01 M EDTA.

Table 7
Determination and recovery of U^{6+} from spiked water samples under the experimental conditions: 50 mL water samples spiked with different amounts of U^{6+} in μg, pH 4, flow rate 2 mL/min and eluent; 10 mL of 1 M HCl, flow rate 0.2 mL/min.

Sample	Added U^{6+} (μg/mL)	Found U^{6+} (μg/mL)	Recovery of U^{6+} (%) ± RSD
Tap water	0.5	0.494 ± 0.005	98.8 ± 0.9
	1.0	1.001 ± 0.005	100.1 ± 0.5
Well water	0.5	0.493 ± 0.007	98.7 ± 1.3
	1.0	0.997 ± 0.007	99.7 ± 0.7
Sea water	0.5	0.497 ± 0.005	99.4 ± 1.0
	1.0	1.003 ± 0.005	100.3 ± 0.5

Table 8
Determination and recovery of U^{6+} from uranmicrolite ore tailings.

Sample	U^{6+} found by ICP-AES ($\mu g\ g^{-1}$)	U^{6+} found by developed method ($\mu g\ g^{-1}$)	Recovery of U^{6+} (%) ± RSD
Uranmicrolite ore tailings	56.34	56.13 ± 0.34	99.6 ± 0.6

data were analyzed according to the linear form of the plot was shown in Fig. 9d and values of B, b and A were calculated as 11.811, 209.9 J/mol and 0.0535 L/g, respectively. The higher value of R^2 (0.9936) suggests that the fall in the heat of sorption was linear not logarithmic. The value for Temkin constant b was positive which indicated that the adsorption process was exothermic.

The Dubinin-Radushkevich isotherm model is applied to estimate the mean free energy of adsorption (E) [59]. If the value of E is between 8 and 16 kJ/mol, the adsorption process is assumed to involve chemical sorption while <8 kJ/mol indicate that the adsorption process is of a physical nature [60]. The linearized D-R isotherm is given by Eq. (9) where q_e is amount of U^{6+} sorbed by EIR at equilibrium (mg/g), q_s is theoretical isotherm saturation capacity (mg/g), K_{ad} (mol^2/kJ^2) and ε are D-R isotherm constants. Here, $\varepsilon = RT\ln((1 + (1/C_e))$ and R, T and C_e represent the universal gas constant (8.314 J/mol K), absolute temperature (K) and adsorbate equilibrium concentration (mg/L), respectively. The intercept of the plot of log q_e versus ε^2 as shown in Fig. 9e gave the value of q_s and the slope yielded the K_{ad} as shown in Table 5. The q_s value calculated using D-R isotherm is 16.44 mg/g is in good agreement with experimental sorption capacity 15.98 mg/g. Therefore D-R isotherm is best suited isotherm model to explain the sorption behaviour of U^{6+} by EIR.

$$\ln q_e = \ln q_s - K_{ad}\varepsilon^2 \quad (9)$$

3.5. Analytical applications

3.5.1. Analysis of synthetic samples

To assess the method applicability for separation and determination of U^{6+} at trace levels from complex mixtures, some synthetic samples were analyzed for determination and recovery of U^{6+} by the recommended column procedure under optimized conditions. Results in Table 6 indicated that U^{6+} could be quantitatively separated i.e. determined from complex matrices i.e. synthetic samples with a relative standard deviation (RSD) of 1.3%. As in some extent, Th^{4+} was co-extracted with U^{6+} so its separation was achieved by masking Th^{4+} in aqueous phase using 1 mL of 0.01 M EDTA [40,61].

3.5.2. Analysis of spiked water samples

Validity of proposed method was judged by analyzing different spiked water samples. All water samples were iso-kinetically collected in polyethylene bottles from different areas of Jalgaon and Mumbai, Maharashtra (India) and filtered through a membrane filter with a pore size of 0.45 mm [48]. Then appropriate volumes of filtered water samples were spiked with different amounts of standard U^{6+} solution and subjected to follow developed method for the determination of U^{6+}. The determination and recovery of U^{6+} is reported in Table 7 which shows quantitative recoveries of U^{6+} from all spiked samples (98.7–100.3%).

3.5.3. Analysis of Uranmicrolite ore tailings

The dried ore tailings (1.0 g) was fused with 3 g of KOH in a nickel crucible for 20 min. The fused mass was cooled and extracted with dilute HNO_3, filtered and diluted to 100 mL [41,62]. Then a known amount of sample solution was passed through the column under the optimized condition for the determination of U^{6+}. The determination and recovery of U^{6+} was quantitative as shown in Table 8. The matrix elements Nb^{5+}, Ta^{5+} and Sb^{3+} in sample did not interfere as their tolerance limits were higher cf. Table 3.

3.6. Comparison with other methods

The analytical characteristics of EIR sorbent for selective SPE and determination of U^{6+} were compared with literature reported methods as shown in Table 9. From Table 9, the reusability of EIR sorbent for U^{6+} was relatively high when compared with other sorbents [10,37,39,41–43] indicated major advantage of impregnation of solid extractor on/in resin. Extraction pH was also one of the main characteristic of the developed method as acidic pH has more advantageous over neutral pH because majority of real samples for U^{6+} remain acidic. Compared to other reported methods, extraction pH of developed method is on more acidic side [2,10,14,16,23,37,39,44]. Preconcentration factor of developed method was also superior to other reported methods [2,41].

4. Conclusion

The present study confirmed that Amberlite XAD-4 resin could be modified by means of impregnation of extractant IMP and characterized. The characterization of EIR showed heterogeneous surface where the extractant IMP arranged itself in such a manner that hydrophilic head of extractant remained free for sorption of U^{6+}. U^{6+} is quantitatively sorbed at pH 4 with flow rate 2 mL/min with recovery of 98.9%. Theoretical isotherm saturation capacity (q_s) calculated using D-R isotherm is 16.44 mg/g for EIR for U^{6+}. The kinetics of the process is well described using Lagergren pseudo first order model. Based on the results of the present work, the prepared EIR may be used as promising

Table 9
Comparison of analytical characteristics of various adsorbents used for U^{6+} extraction.

Sorbent	pH	Reusability	LOD[a] (μg/L)	PF[b]	Ref.
Imprinted magnetic composites	5.0	–	–	120	[2]
Carboxylate-functionalized poly(hydroxyethylmethacrylate)-grafted lignocellulosics	6.0	2–4	–	–	[10]
β-Cyclodextrin/$Al(OH)_3$ composites	6.0	–	–	–	[14]
Dopamine-functionalized SBA-15	6.0	–	–	–	[16]
Multiwalled carbon nanotubes	5.0	–	–	–	[23]
Pyridylazo resorcinol - functionalized amberlite XAD-16	4.5	30	–	–	[37]
Quinizarin impregnated amberlite XAD-16	6.0–8.0	40–50			
1.6×10^{-9} M	–	[39]			
Cyanex272 impregnated on amberlite XAD-2	1×10^{-3} M HNO_3	>50	10.5	>100	[41]
Cyanex272 resin impregnated amberlite XAD-2	1×10^{-3} M HNO_3	50	0.6	>500	[42]
Carminic acid impregnated Amberlite XAD-16 resin	3.75–6.50	>50	0.18	200	[44]
Isonitroso-4-methyl-2-pentanone impregnated amberlite XAD-4	4.0	80	0.24	150	Present work

[a] LOD: Limit of detection.
[b] PF: Preconcentration factor.

adsorbent for the treatment of wastewaters containing U^{6+} and for separation, determination of U^{6+} from complex matrix.

Acknowledgements

One of the author (S.R.T.) is grateful to the University Grant Commission (UGC), India for the financial support given via the Research Fellowship in Science for Meritorious Students (RFSMS) vide letter no. F.7-136/2007(BSR), dated 19/10/2012.

References

[1] M. Solgy, M. Taghizadeh, D. Ghoddocynejad, Adsorption of uranium(VI) from sulphate solutions using Amberlite IRA-402 resin: equilibrium, kinetics and thermodynamics study, Ann. Nucl. Energy 75 (2015) 132–138.
[2] J. Qian, S. Zhang, Y. Zhou, P. Dong, D. Hua, Synthesis of surface ion-imprinted magnetic microspheres by locating polymerization for rapid and selective separation of uranium(VI), RSC Adv. 5 (2015) 4153–4161.
[3] J.S. Santos, L.S.G. Teixeira, W.N.L. Dos Santos, V.A. Lemos, J.M. Godoye, S.L.C. Ferreira, Uranium determination using atomic spectrometric techniques: an overview, Anal. Chim. Acta 674 (2010) 143–156.
[4] M. Sprynskyy, T. Kowalkowski, H. Tutu, E.M. Cukrowska, B. Buszewski, Ionic liquid modified diatomite as a new effective adsorbent for uranium ions removal from aqueous solution, Colloids Surf. A Physicochem. Eng. Asp. 465 (2015) 159–167.
[5] X. Zhu, S.D. Alexandratos, Development of a new ion-exchange/coordinating phosphate ligand for the sorption of U(VI) and trivalent ions from phosphoric acid solutions, Chem. Eng. Sci. 127 (2015) 126–132.
[6] Agency for Toxic Substances & Disease Registry (ATSDR), Uranium toxicity, Web page link:, . http://www.atsdr.cdc.gov/csem/csem.asp?csem=16&po=0 (accessed on 06th September 2016).
[7] World Health Organization (WHO), The chemical toxicity of uranium, Web page link:, . http://www.who.int/ionizing_radiation/pub_meet/en/Depluranium4.pdf (accessed on 06th September 2016).
[8] C. Nuccetelli, M. Grandolfo, S. Risica, Depleted uranium: possible health effects and experimental issues, Microchem. J. 79 (2005) 331–335.
[9] G.V. Britsom, B. Slowikowski, M. Bickel, A rapid method for the detection of uranium in surface water, Sci. Total Environ. 173 (174) (1995) 83–89.
[10] T.S. Anirudhan, L. Divya, P.S. Suchithra, Kinetic and equilibrium characterization of uranium(VI) adsorption onto carboxylate-functionalized poly(hydroxyethylmethacrylate)-grafted lignocellulosics, J. Environ. Manag. 90 (2009) 549–560.
[11] T.P. Rao, P. Metilda, J.M. Gladis, Preconcentration techniques for uranium(VI) and thorium(IV) prior to analytical determination-an overview, Talanta 68 (2008) 1047–1064.
[12] R.A.A. Muzzarelli, Potential of chitin/chitosan-bearing materials for uranium recovery: An interdisciplinary review, Carbohydr. Polym. 84 (2011) 54–63.
[13] J. Kim, C. Tsouris, R.T. Mayes, Y. Oyola, T. Saito, C.J. Janke, S. Dai, E. Schneider, D. Sachde, Recovery of uranium from seawater: A review of current status and future research needs, Sep. Sci. Technol. 48 (2013) 367–387.
[14] C. Ding, W. Cheng, Z. Jin, Y. Sun, Plasma synthesis of β-cyclodextrin/$Al(OH)_3$ composites as adsorbents for removal of UO_2^{2+} from aqueous solutions, J. Mol. Liq. 207 (2015) 224–230.
[15] Y. Sun, S. Yang, Y. Chen, C. Ding, W. Cheng, X. Wang, Adsorption and desorption of U(VI) on functionalized graphene oxides: A combined experimental and theoretical study, Environ. Sci. Technol. 49 (2015) 4255–4262.
[16] J.K. Gao, L.A. Hou, G.H. Zhanga, P. Gu, Facile functionalized of SBA-15 via a biomimetic coating and its application in efficient removal of uranium ions from aqueous solution, J. Hazard. Mater. 286 (2015) 325–333.
[17] W. Cheng, M. Wang, Y. Zhiguo, Y. Sun, C. Ding, The efficient enrichment of U(VI) by graphene oxide-supported chitosan, RSC Adv. 4 (2014) 61919–61926.
[18] S. Biswas, P.N. Pathak, D.K. Singh, S.B. Roy, V.K. Manchanda, Evaluation of dinonyl phenyl phosphoric acid (DNPPA) and its synergistic mixtures with neutral oxodonors for extraction and recovery of uranium from nitric acid medium, Int. J. Miner. Process. 104-105 (2012) 17–23.
[19] J.C.B.S. Amaral, C.A. Morais, Thorium and uranium extraction from rare earth elements in monazite sulfuric acid liquor through solvent extraction, Miner. Eng. 23 (2010) 498–503.
[20] G. Hellé, C. Mariet, G. Cote, Liquid-liquid extraction of uranium(VI) with Aliquats 336 from HCl media in microfluidic devices: combination of micro-unit operations and online ICP-MS determination, Talanta 139 (2015) 123–131.
[21] V. Stucker, J. Ranville, M. Newman, A. Peacock, J. Cho, K. Hatfield, Evaluation and application of anion exchange resins to measure groundwater uranium flux at a former uranium mill site, Water Res. 45 (2011) 4866–4876.
[22] F. Semnani, Z. Asadi, M. Samadfam, H. Sepehrian, Uranium(VI) sorption behavior onto amberlite CG-400 anion exchange resin: effects of pH, contact time, temperature and presence of phosphate, Ann. Nucl. Energy 48 (2012) 21–24.
[23] I.I. Fasfous, J.N. Dawoud, Uranium(VI) sorption by multiwalled carbon nanotubes from aqueous solution, Appl. Surf. Sci. 259 (2012) 433–440.
[24] Q. Song, L. Ma, J. Liu, C. Bai, J. Geng, H. Wang, B. Li, L. Wang, S. Li, Preparation and adsorption performance of 5-azacytosine-functionalized hydrothermal carbon for selective solid-phase extraction of uranium, J. Colloid Interface Sci. 386 (2012) 291–299.
[25] J. Fasihi, M. Shamsipur, A. Khanchi, M. Mahani, K. Ashtari, Imprinted polymer grafted from silica particles for on-line trace enrichment and ICP-OES determination of uranyl ion, Microchem. J. 126 (2016) 316–321.
[26] D.K. Kulal, A.V. Pansare, S.R. Tetgure, M. Karve, V.R. Patil, Determination of uranium(VI) using *Penicillium chrysogenum* immobilized on silica gel and spectrophotometer, J. Radioanal. Nucl. Chem. 307 (2016) 1253–1263.
[27] R. Rodríguez, J. Avivar, L.O. Leal, V. Cerdà, L. Ferrer, Strategies for automating solid-phase extraction and liquid-liquid extraction in radiochemical analysis, TrAC, Trends Anal. Chem. 76 (2016) 145–152.
[28] S.J. Ahmadi, O.N. Kalkhoran, S.S. Arani, Synthesis and characterization of new ion-imprinted polymer for separation and preconcentration of uranyl (UO_2^{2+}) ions, J. Hazard. Mater. 175 (2010) 193–197.
[29] T.E. Milja, K.P. Prathish, T.P. Rao, Synthesis of surface imprinted nanospheres for selective removal of uranium from simulants of Sambhar salt lake and ground water, J. Hazard. Mater. 188 (2011) 384–390.
[30] D. James, G. Venkateswaran, T.P. Rao, Removal of uranium from mining industry feed simulant solutions using trapped amidoxime functionality within a mesoporous imprinted polymer material, Microporous Mesoporous Mater. 119 (2009) 165–170.
[31] E. Constantinou, I. Pashalidis, Uranium determination in water samples by liquid scintillation counting after cloud point extraction, J. Radioanal. Nucl. Chem. 286 (2010) 461–465.
[32] A. Saha, S.B. Deb, A. Sarkar, M.K. Saxena, B.S. Tomar, Simultaneous preconcentration of uranium and thorium in aqueous samples using cloud point extraction, RSC Adv. 6 (2016) 20109–20119.
[33] I.M.M. Rahman, Z.A. Begum, H. Hasegawa, Selective separation of elements from complex solution matrix with molecular recognition plus macrocycles attached to a solid-phase: A review, Microchem. J. 110 (2013) 485–493.
[34] L. Dolatyari, M.R. Yaftian, S. Rostamnia, Removal of uranium(VI) ions from aqueous solutions using Schiff base functionalized SBA-15 mesoporous silica materials, J. Environ. Manag. 169 (2016) 8–17.
[35] D. Yuan, C. Long, X. Xin, L. Yuan, S. Liao, Y. Wang, Removal of uranium(VI) from aqueous solution by amidoxime functionalized superparamagnetic polymer microspheres prepared by a controlled radical polymerization in the presence of DPE, Chem. Eng. J. 285 (2016) 358–367.
[36] L. Shao, X. Wang, Y. Ren, S. Wang, J. Zhong, M. Chu, H. Tang, L. Luo, D. Xie, Facile fabrication of magnetic cucurbit[6]uril/graphene oxide composite and application for uranium removal, Chem. Eng. J. 286 (2016) 311–319.
[37] M.F. Cheira, Synthesis of pyridylazo resorcinol functionalized Amberlite XAD-16 and its characteristics for uranium recovery, J. Environ. Chem. Eng. 3 (2015) 642–652.
[38] A. Ahmad, J.A. Siddique, M.A. Laskar, R. Kumar, S.H. Mohd-Setapar, A. Khatoon, R.A. Shiekh, New generation Amberlite XAD resin for the removal of metal ions: A review, J. Environ. Sci. 31 (2015) 104–123.
[39] M.S. Hosseini, A.H. Bandegharaei, Comparison of sorption behavior of Th(IV) and U(VI) on modified impregnated resin containing quinizarin with that conventional prepared impregnated resin, J. Hazard. Mater. 190 (2011) 755–765.
[40] B.N. Singh, B. Maiti, Separation and preconcentration of U(VI) on XAD-4 modified with 8-hydroxy quinolone, Talanta 69 (2006) 393–396.
[41] M. Karve, K. Pandey, Cyanex272 impregnated on Amberlite XAD-2 for separation and preconcentration of U(VI) from uranmicrolite (leachates) ore tailings, J. Radioanal. Nucl. Chem. 285 (2010) 627–633.
[42] M. Karve, R.V. Rajgor, Amberlite XAD-2 impregnated organophosphinic acid extractant for separation of uranium(VI) from rare earth elements, Desalination 232 (2008) 191–197.
[43] M.S. Hosseini, A.H. Bandegharaei, Selective extraction of Th(IV) over U(VI) and other co-existing ions using eosin B-impregnated Amberlite IRA-410 resin beads, J. Radioanal. Nucl. Chem. 283 (2010) 23–30.
[44] A.H. Bandegharaei, M.S. Hosseini, Y. Jalalabadi, M. Nedaie, M. Sarwghadi, A. Taherian, E. Hosseini, A novel extractant-impregnated resin containing carminic acid for selective separation and pre-concentration of uranium(VI) and thorium(IV), Int. J. Environ. An. Ch. 93 (2013) 108–124.
[45] K. Babić, G.H.M. Driessen, A.G.J. van der Ham, A.B. de Haan, Chiral separation of amino-alcohols using extractant impregnated resins, J. Chromatogr. A 1142 (2007) 84–92.
[46] K. Babić, L. van der Ham, A. de Haan, Recovery of benzaldehyde from aqueous streams using extractant impregnated resins, React. Funct. Polym. 66 (2006) 1494–1505.
[47] A.R. Sani, A.H. Bandegharaei, S.H. Hosseini, K. Kharghani, H. Zarei, A. Rastegar, Kinetic, equilibrium and thermodynamic studies on sorption of uranium and thorium from aqueous solutions by a selective impregnated resin containing carminic acid, J. Hazard. Mater. 286 (2015) 152–163.
[48] S.R. Tetgure, D.J. Garole, A.U. Borse, A.D. Sawant, Novel extractant impregnated resin for thorium preconcentration from different environmental samples-column and batch study, Sep. Sci. Technol. 50 (2015) 2496–2508.
[49] D.J. Garole, S.R. Tetgure, A.U. Borse, Y.R. Toda, V.J. Garole, B.R. Sankapal, P.K. Baviskar, The first report on SILAR deposited nanostructured uranyl sulphide thin films and their chemical conversion to silver sulphide, New J. Chem. 39 (2015) 8695–8702.
[50] A.I. Vogel, A Text Book of Quantitative Inorganic Analysis, 3rd edn. Longman, London, UK, 1962.
[51] F.D. Snell, Photometric and Fluorometric Methods of Analysis of Metals, John Wiley and Sons, New York, USA, 1978.
[52] M.F. Fathalla, S.N. Khattab, Spectrophotometric determination of pK_a's of 1-hydroxybenzotriazole and oxime derivatives in 95% acetonitrile-water, J. Chem. Soc. Pak. 33 (2011) 324–332.
[53] S.S. Rodríguez, J.T. Reyes, E.G. Segura, M.S. Ríos, A.C. Cruz, Removal of indigo carmine by a Ni nanoscale oxides/*Schoenoplectus acutus* composite in batch and fixed bed column systems, Sep. Sci. Technol. 50 (2015) 1602–1610.

[54] S. Lagergren, About the theory of so-called adsorption of soluble substances, Kungliga Svenska Vetenskapsakademiens, Handlingar, Band 24 (1898) 1–39.
[55] T. Sreenivas, K.C. Rajan, Studies on the separation of dissolved uranium from alkaline carbonate leach slurries by resin-in-pulp process, Sep. Purif. Technol. 112 (2013) 54–60.
[56] C. Chen, J. Wang, Uranium removal by novel graphene oxide-immobilized *Saccharomyces cerevisiae* gel beads, J. Environ. Radioact. 162–163 (2016) 134–145.
[57] W.J. Weber, J.C. Morris, Kinetics of adsorption on carbon from solution, J. Sanit. Eng. Div. ASCE 89 (1963) 31–60.
[58] H. Heshmati, M.T. Mostaedi, H.G. Gilani, A. Heydari, Kinetic, isotherm, and thermodynamic investigations of uranium(VI) adsorption on synthesized ion-exchange chelating resin and prediction with an artificial neural network, Desalin. Water Treat. 55 (2015) 1076–1087.
[59] M.M. Dubinin, Molecular sieves-II, Chapter 1: Investigations of equilibria and kinetics of adsorption of gases on zeolites, 1977. ACS Symposium Series 40, 1977, pp. 1–15, http://dx.doi.org/10.1021/bk-1977-0040.ch001 (Chapter DOI:).
[60] N. Samadi, R. Hasanzadeh, M. Rasad, Adsorption isotherms, kinetic, and desorption studies on removal of toxic metal ions from aqueous solutions by polymeric adsorbent, J. Appl. Polym. Sci. 132 (2015) 41642–41654.
[61] M. Shamsipur, A.R. Ghiasvand, Y. Yamini, Solid-phase extraction of ultratrace uranium(VI) in natural waters using octadecyl silica membrane disks modified by tri-n-octylphosphine oxide and its spectrophotometric determination with dibenzoylmethane, Anal. Chem. 71 (1999) 4892–4895.
[62] W.F. Hillebrand, G.E.F. Lundell, Applied Inorganic Analysis of Metal, Minerals and Rocks, Wiley, New York, USA, 1953.